Supramolecular Chemistry
Publication details, including instructions for authors and subscription information:
http://www.informaworld.com/smpp/title~content=t713649759

DNA conjugates bearing a ferrocenyl group in backbone and their electrochemical behaviour

Toshihiro Ihara[a]; Daisuke Sasahara[a]; Masamichi Shimizu[a]; Akinori Jyo[a]
[a] Department of Applied Chemistry and Biochemistry, Graduate School of Science and Technology, Kumamoto University, Kumamoto, Japan

To cite this Article Ihara, Toshihiro , Sasahara, Daisuke , Shimizu, Masamichi and Jyo, Akinori(2009) 'DNA conjugates bearing a ferrocenyl group in backbone and their electrochemical behaviour', Supramolecular Chemistry, 21: 3, 207 — 217
To link to this Article: DOI: 10.1080/10610270802468405
URL: http://dx.doi.org/10.1080/10610270802468405

Supramolecular Chemistry
Vol. 21, Nos. 3–4, April–June 2009, 207–217

Taylor & Francis
Taylor & Francis Group

DNA conjugates bearing a ferrocenyl group in backbone and their electrochemical behaviour

Toshihiro Ihara*, Daisuke Sasahara, Masamichi Shimizu and Akinori Jyo

Department of Applied Chemistry and Biochemistry, Graduate School of Science and Technology, Kumamoto University, Kumamoto, Japan

(*Received 2 July 2008; final version received 8 September 2008*)

Ferrocene (Fc)-based amidite reagents with three different chain lengths were synthesised. Using these amidites, a Fc unit was built into the backbone of each oligonucleotide to synthesise 9 Fc-DNA conjugates, FcDNAs. While Fc units in duplex backbone destabilised the structures, those in hairpin loop could stabilise hairpin structures, if the chain length is appropriate. The shifts in the oxidation potentials of Fc units in DNAs were opposite each other for duplex and hairpin formations; the potentials of the Fc in duplex backbones shifted to negative side, and that in hairpin loop positive side. This would be explained by the difference in hydrophilicity of the microenvironments, where each Fc is located.

Keywords: DNA conjugate; ferrocene; amidite reagent; duplex; hairpin

Introduction

Covalent connection between two or more molecules is a smart way for producing the novel molecules possessing combined and synergistic properties, so-called conjugates. Many natural molecules such as nucleic acids and proteins have been subjected to conjugation with various other natural and synthetic molecules according to the demand (*1*, *2*). One of the most successful works on proteins should be that for antibody-enzyme conjugates, which are, now, commonly used in non-radioactive enzyme-linked immunosorbent assay techniques in immunoassay. The conjugation of nucleic acids, DNAs and RNAs, with certain chemical groups has also studied and provided the unique nucleic acid conjugates having carefully engineered characteristics such as DNA cleaving activity (*3*), catalytic activity of certain reaction (*4*), fluorescent property (*5*) or electrochemical activity (*6*) for DNA probing and so on.

Electrochemical techniques are potentially sensitive and versatile. The redox reaction of DNA is, however, irreversible and occurs at highly negative and positive potentials in which sensitive detection of the feeble current is difficult because of large background current coming from solvent decomposition. Therefore, such conjugate should be useful as an electrochemically active DNA probe that undergoes reversible electrode reactions at less-extreme potentials. We have already proposed the methods for electrochemical detection of DNA by using ferrocene (Fc)-modified oligonucleotide as a probe, in which femto mole detection of the target was attainable on HPLC equipped with electrochemical detector (*7*). The same probe was also applied in the system of the first electrochemical gene sensor (*8–10*), in which sandwich-type tandem duplex consisting of the Fc probe, single-stranded target, and the immobilised capture probe formed on the electrode surface. Since, then, electrochemical studies on DNA-related interactions have been drawing much attention (*11–16*). Quite elaborated systems have been constructed for genotyping and sensing of certain chemical species such as metal ions (*17*) and proteins (*18–20*).

Most of the probes used in these studies were the DNA conjugates carrying a redox-active molecule on one of their termini. We are interested in the electrochemical behaviour of the molecules built in the middle of DNA backbone (*21*). The microenvironment of the certain point in a DNA backbone should change depending on the second structure, where it is located (Figure 1). If the redox-active molecules built in a DNA backbone act as the probe for second structures, they would be very useful for the fundamental studies of functional nucleic acids such as ribozyme, DNAzyme and aptamer, because 'right' higher-ordered structure is critical for them to function (*22*, *23*).

It is known that the redox potential of the Fc unit that is tethered to 5′-end of DNA significantly shifts when it is packed in confined space on an electrode surface (*9*, *10*, *24*). Therefore, Fc would be expected to be a probe responding to microenvironment. Here, we synthesised three Fc-based amidite reagents with various lengths of linker chains to prepare DNA conjugates carrying an Fc unit in their backbone (FcDNA conjugates). The effect of insertion of an Fc unit in DNA backbone was studied in terms of the

*Corresponding author. Email: toshi@chem.kumamoto-u.ac.jp

ISSN 1061-0278 print/ISSN 1029-0478 online

DOI: 10.1080/10610270802468405
http://www.informaworld.com

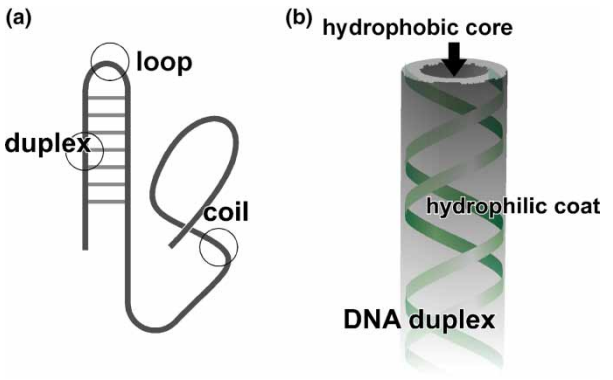

Figure 1. Microenvironments form around DNA. (a) A single-stranded DNA or RNA form various second structures such as duplexes, triplexes, quadruplexes, loops and coils; (b) DNA duplex could be assumed as a concentric double-layered cylinder consisting of hydrophobic core of base-pair stacking and hydrophilic coat of phosphodiester backbone.

thermal stability of hairpin and duplex structures. Electrochemical responses were examined for each structure by cyclic voltammetry (CV).

Results and discussion

Synthesis of Fc amidites

Three Fc-based amidite reagents with the linker chains of different lengths, **7**, **10** and **14**, were synthesised according to Schemes 1 and 2. Generally a diol is the key compound when one designs the synthetic scheme of an amidite reagent. One of its hydroxyl groups is tritylated by 4,4′-dimethoxytrityl chloride (DMTr-Cl), and then the other is phosphitylated by chloro(diisopropylamino)(β-cyanoethoxy)phosphine to form the desired structure of amidite reagent directly used for an automated DNA synthesizer. Here, the Fc diol (**5**) was synthesised as the common intermediate for the three amidites.

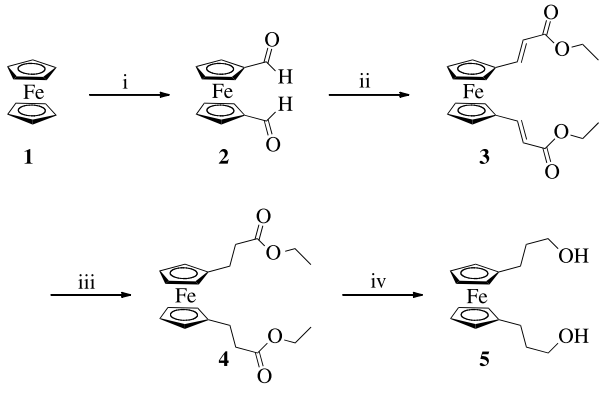

Scheme 1. (i) (1) TMEDA, *n*-BuLi, Hexane, rt, 24 h, (2) DMF, THF, − 78°C, 22 h (76%); (ii) diethyl phosphoacetate, NaH, THF, rt, 4 h (97%); (iii) CuCl, $NaBH_4$, MeOH, 0°C, 7 h (84%); (iv) LAH, THF, reflux, 4 h (84%).

Fc diol (**5**) was prepared in four steps from Fc (**1**) basically according to the procedures previously described (*25–30*). The intermediates (**2**, **3** and **4**) were obtained in reasonable yields, 76, 97 and 84%, respectively. Fc diol (**5**) was obtained by reduction of **4** with lithiumaluminium-hydride (LAH) in 84% yield. Overall, yield of **5** from **1** was 52%.

The amidite reagent with short linker chain (**7**) was directly synthesised from **5** by tritylation of one of the hydroxyl group with DMTr-Cl (*31*) and then phosphitylation of other hydroxyl group with chloro(diisopropylamino)(β-cyanoethoxy)phosphine (*27*). The yields of these successive two reactions were 46 (**6**) and 84% (**7**), respectively. The amidite with medium linker chain (**10**) was obtained by chain elongation by Williamson ether synthesis with the assistance of 15 Crown 5 (*32–35*) and successive phosphitylation with chloro(diisopropylamino)(β-cyanoethoxy)phosphine (*27*) in yields of 44 (**9**) and 83% (**10**), respectively. The amidite with long linker chain (**14**) was synthesised in three step reactions. First, both linkers chains of **5** were elongated by Williamson synthesis with **11** using 15 Crown 5 to form the ditritylated Fc derivative with long linker chain (**12**) in yield of 42% (*32–35*). Then, one of the dimethoxytrityl groups was selectively removed using Lewis acid, $Ce(OTf)_4$ to form monotrityl compound (**9**) in good yield, 91% (*36*). Finally, **9** was phosphitylated with chloro(diisopropylamino)(β-cyanoethoxy)phosphine in yield of 99% (*27*). Thus, we could prepare all the amidite reagents (**7**, **10** and **14**) in reasonable yields with sufficient purity for the use of an automated DNA synthesizer.

Synthesis of FcDNA conjugates

FcDNA conjugates having an Fc unit in a backbone and unmodified oligonucleotides used in this study are shown in Figure 2(a), (b). 'S', 'M' and 'L' in the names of the conjugates stand for the lengths of the linker chain, short, medium and long, respectively, of an Fc unit in each strand. 'd' and 'h' stand for the second structures, duplex and hairpin, respectively, which each strand is supposed to form. The numbers indicate the number of nucleotide units. The conjugates were synthesised using the standard procedure with an automated DNA synthesizer. The yields of the coupling step of all Fc amidites were more than 80%. All oligonucleotides were purified with the conventional two-step procedure using RP-HPLC (*2*, *37*). The chromatograms showed that the purities of all oligonucleotides including FcDNAs were satisfactory (>99%). All of them were identified with MALDI-TOF mass spectrometry.

Thermal stabilities of hairpin and duplex structures

Duplex structure

The effect of Fc unit insertion into a DNA backbone on duplex stability was studied by UV melting experiments

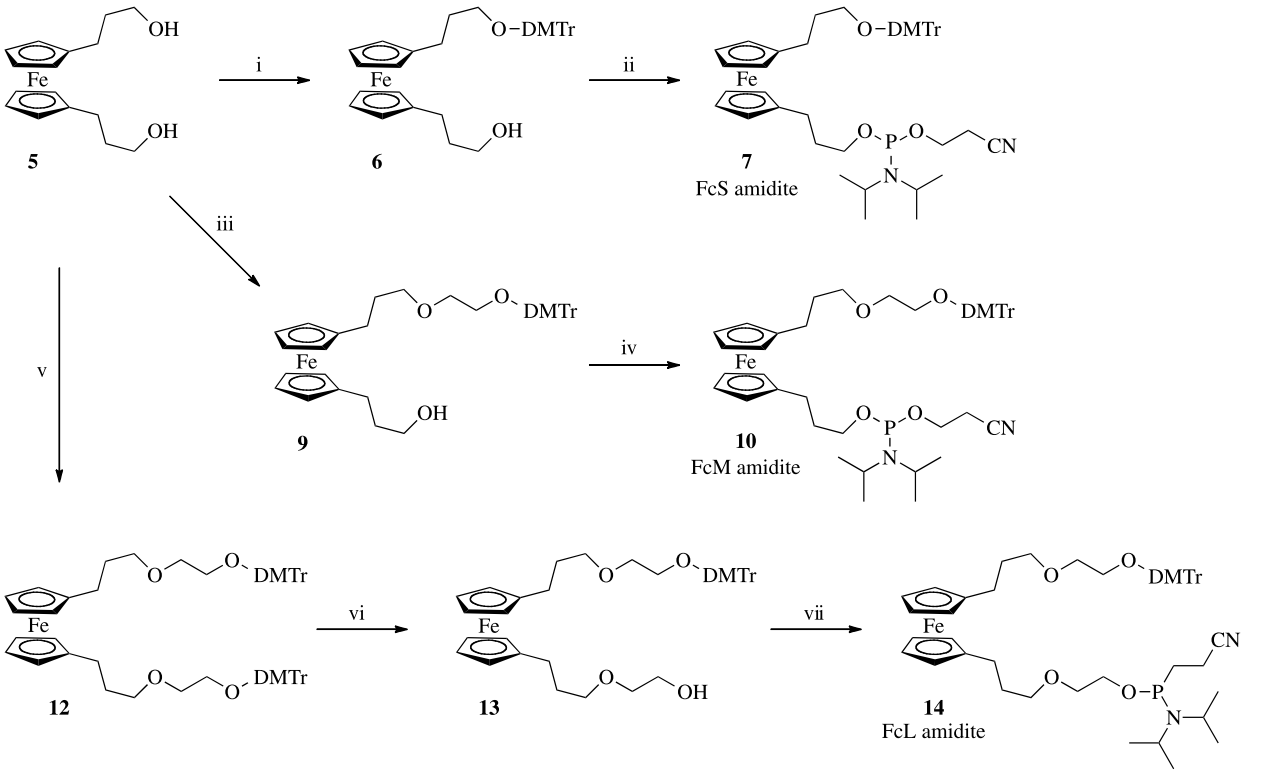

Scheme 2. (i) DMAP, DIPEA, DMTr-Cl, THF, rt, 4 h (46%); (ii) DIPEA, $ClP(iPr_2N)(OCH_2CH_2CN)$, CH_3CN, rt, 30 min (83%); (iii) NaH, 15C5, ICH_2CH_2DMTr (**8**), THF, reflux, 37 h (44%); (iv) DIPEA, $ClP(iPr_2N)(OCH_2CH_2CN)$, CH_3CN, rt, 30 min (84%); (v) NaH, 15C5, $BrCH_2CH_2DMTr$ (**11**), THF, reflux, 25 h (42%); (vi) $Ce(OTf)_3$, H_2O, CH_3CN, rt, 24 h (91%); (vii) DIPEA, $ClP(iPr_2N)$-(OCH_2CH_2CN), CH_3CN, rt, 30 min (84%) (99%).

of the six duplexes with FcDNA conjugates (**FcSd14**, **FcMd14** and **FcLd14**) (*37*). Two groups of the duplexes were built and examined for their thermal stability. In the duplexes with **cd15**, a cytosine (C) is located at the same position with the Fc unit on the opposite strand. Therefore, one unpaired C-Fc is located at the centre of the each duplex. In another group of the duplexes, the cytosine is deleted from **cd14**. Fc units have no other choice other than to flip out (bulge out) from the duplexes with **cd14**. All the duplexes cooperatively dissociated at once. The normalised UV melting curves of the duplexes **d15/cd15** and **FcLd14/cd15** were shown in Figure 3(a) as representatives. T_{max}s (T_{max}: the temperature given by the maximum of the first derivative of each melting curve) for all eight duplexes were shown in Table 1. All Fc units in DNA conjugates apparently destabilised their duplex structures. Flexible structure of the Fc unit inserted at the centre of 14-mer oligonucleotide breaks the continuity of the sequence to separate into two 7-mer blocks. That is, the formation of the duplexes with FcDNA conjugates would be accompanied by large entropic penalty compared with that of the control duplex, **d15/cd15**. This tendency became more significant for the Fc units with longer linker chains because of their higher flexibility. This was true for the duplexes with Fc bulges (with **cd14**).

Hairpin structure

The stabilities of hairpin structures of FcDNA conjugates were also evaluated by UV melting experiments (*37*). Fc units were built in the loop moieties of the hairpins with three base-pairs (**FcSh6**, **FcMh6** and **FcLh6**) and four base-pairs (**FcSh8**, **FcMh8** and **FcLh8**) stems. The normalised UV melting curves of the hairpins **T_3h8** and **FcMh8** were shown in Figure 3(b) as representatives. T_{max}s for all hairpins containing two controls (**T_3h6** and **T_3h8**) were shown in Table 2. Interestingly, contrary to the case of the duplexes, Fc insertion could stabilise the hairpin structure, when the Fc unit with appropriate linker length is located in a loop position. The Fc units with medium (FcM) and long (FcL) linkers seemed to act as better loops than $(dT)_3$ in **T_3h6** and **T_3h8**. The most suitable length as a hairpin loop seems to be the medium one (FcM) in **FcMh6** or **FcMh8**. Modelling studies showed that the distance between the two terminal oxygen atoms in FcS, FcM and FcL loops was 14, 18.7 and 23.5 Å, respectively, in all of their *trans* conformations. The distance in FcM is the closest one to the diameter of a DNA duplex, 18.1 Å for P–P distance. While the FcM loop would cap one of the ends of the duplex by bridging both strands, the FcS loop would induce a substantial turbulence of the terminal structure of the stem region,

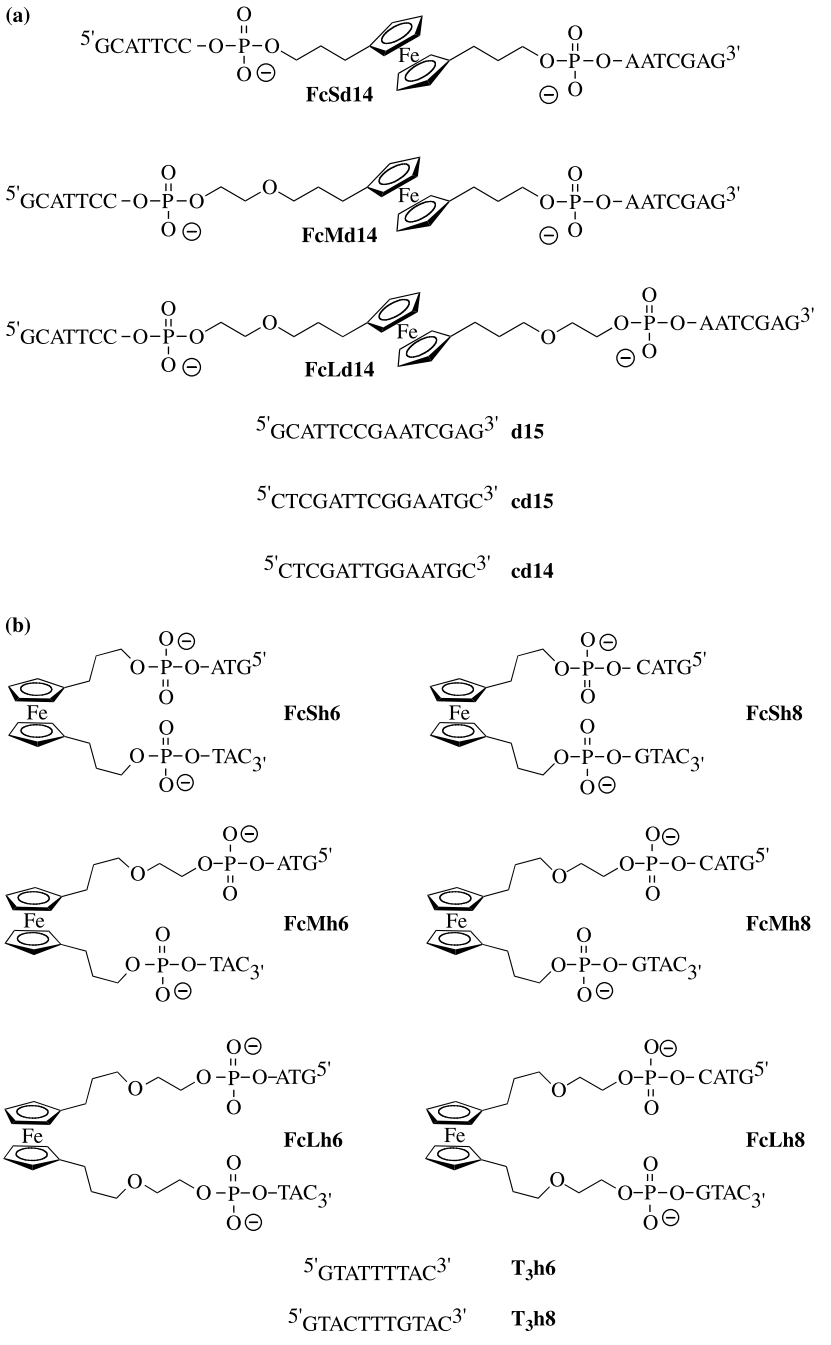

Figure 2. The structures and the sequences of FcDNAs and unmodified oligonucleotides used in the studies for (a) duplex and (b) hairpin formation.

because its length is too short to connect the both strands without strain. On the other hand, FcL loop seems not to be favourable compared with FcM, probably, due to an entropic effect. This effect would become obvious for **FcLh6**, because the thermal stability of the hairpin structure with three base-pairs is less than that of **FcLh8**. One of the possible structures of the **FcMh8** optimised by AMBER* is shown in Figure 4.

Electrochemical behaviour of FcDNA conjugates

The studies of thermal stability showed that Fc units could be allocated on the points we desired. Here, we examined the effect of microenvironment of the second structure, where each Fc is located, on its electrochemical behaviour by CV measurement using microelectrodes. The voltammograms of **FcMh6** measured at 2°C was shown in Figure 5. All other voltammograms obtained here also

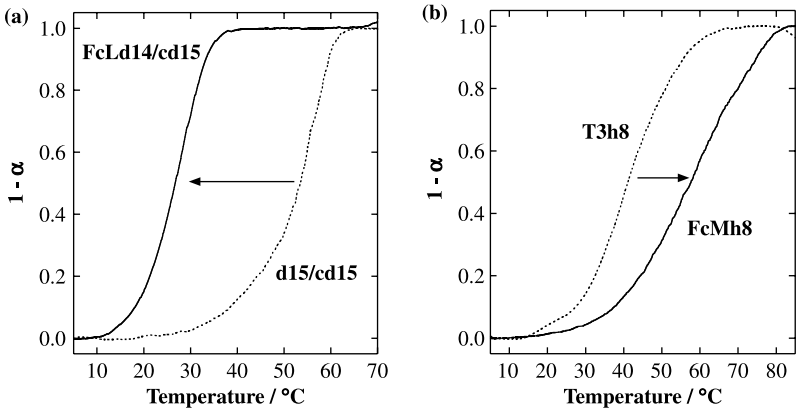

Figure 3. Normalised UV melting curves for the duplexes and hairpins containing FcDNAs measured in phosphate buffer (10 mM, pH 7, 100 mM KCl). (a) Duplexes, **d15/cd15** (broken curve) and **FcL14/cd15** (solid curve); (b) hairpins, **T3h8** (broken curve) and **FcMh8** (solid curve); concentrations of each component of the duplexes or hairpins were 1 μM.

showed sigmoidal shape because of omnidirectional radial diffusion around the microelectrode (*38*). The shifts in the oxidation potentials of Fc units associated with the formation of corresponding structures ($\Delta E_a^{o\prime}$) were summarised in Table 3. For the duplexes, the potentials of **FcSd14**, **FcMd14** and **FcLd14** were measured in the absence and in the presence of complementary oligonucleotides, **cd15** and **cd14**, each of which provides the duplex containing unpaired C-Fc and bulged out Fc, respectively. Hairpin formation was controlled by temperature. CV measurements were carried out for **FcSh8**, **FcMh6** and **FcLh6** at 2 and 50°C, because the hairpin structures of **FcMh8** and **FcLh8** are too stable ($T_{max} = 59.1$°C) to break at the temperature, where CV could be performed using our system.

All the FcDNA conjugates moderately shifted their oxidation potentials when forming the structures. It is very interesting to note that the potentials shifted to opposite side each other for duplex and hairpin; the potentials shifted to negative and positive sides with duplex and hairpin structure formation, respectively. DNA duplex could be assumed as a concentric double-layered cylinder consisting of a hydrophobic core of base-pair stacking and a hydrophilic coat of phosphodiester–sugar backbones (Figure 1(b)). The Fc units in hairpin loop would have no other choice to lie on the top of the hydrophobic core because of their structural restriction. On the other hand, the locations of the Fc units built in duplexes are somewhat uncertain. However, it would be sure that they are located

Table 1. T_{max}s of the duplexes consisting of FcODN and **cd15** or **cd14**.

	T_{max}/°C	
FcDNA	**cd15**	**cd14**
d15	56.1	44.1
FcSd14	39.6	41.5
FcMd14	36.7	38.9
FcLd14	24.7	24.2

Table 2. T_{max}s of the hairpin melting.

FcDNA	T_{max}/°C	FcDNA	T_{max}/°C
T_3h6	–	**T_3h8**	40.6
FcSh6	–	**FcSh8**	11.4
FcMh6	38.1	**FcMh8**	59.1
FcLh6	22.1	**FcLh8**	59.1

–, T_{max}s could not be obtained from melting curves.

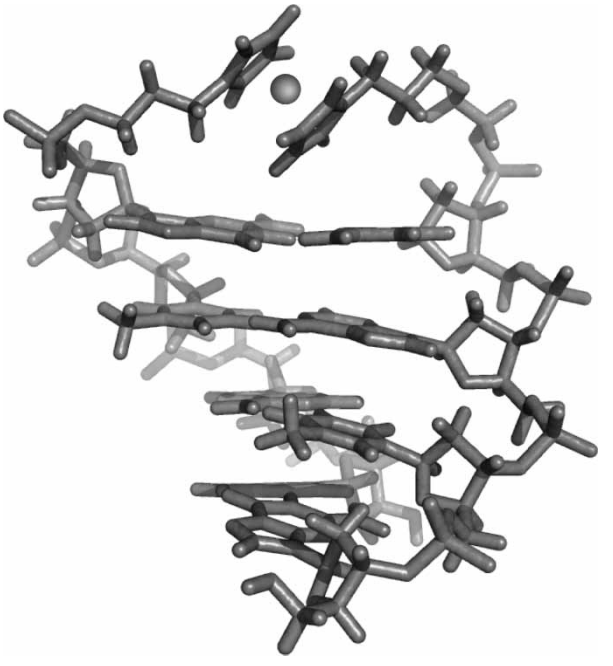

Figure 4. A local minimum structure of **FcMh8** hairpin. The model was geometry-optimised by AMBER* force field with GB/SA (generalised born/surface area) solvent model using MacroModel version 9.1.

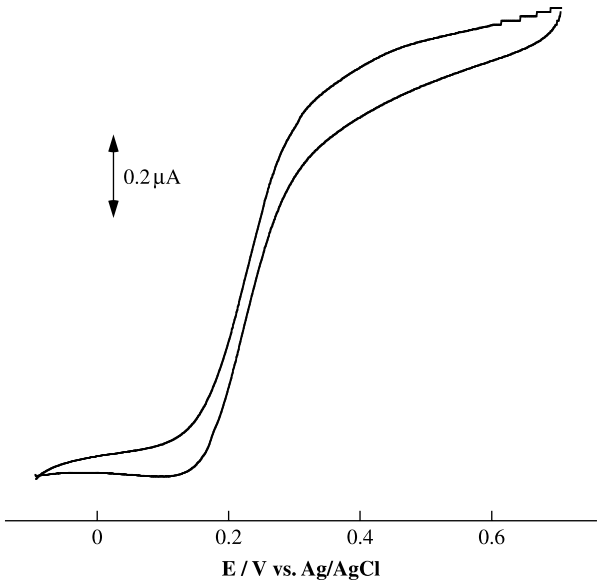

Figure 5. Cyclic voltammogram (dual mode) of **FcMh6** measured at 2°C. The current profile on W_g was shown. DNA solutions (20 μl) containing 10 μM each DNA component [10 mM phosphate buffer (pH 7), 100 mM KCl] were subjected to the measurement. The potential of W_g was scanned at the rate of 10 mV s^{-1} from −0.2 to 0.6 V; W_c was kept constant at −0.2 V.

in more hydrophilic microenvironment than that in hairpin loop. The contrastive electrochemical behaviour observed for the Fc units in both different second structures could be explained simply using the double-layered cylinder model of DNA duplex.

A ferrocenyl cation (Fc^+: oxidised form) in duplex backbone (**FcSd14**, **FcMd14** and **FcLd14**) would be preferred in the microenvironment because of its hydrophilicity and electrostatic interaction with phosphates in backbones. This would explain the shift in the oxidation potential of the Fc to negative side. This effect was more significant for the duplexes with **cd14**, because Fc bulges in the duplexes with **cd14** could expose more to hydrophilic environment of bulk solution. The maximum $\Delta E_a^{o\prime}$ in duplex formation was estimated to be −74 mV for the duplex **FcMd14/cd14**. Considering the thermodynamic cycle consisting of redox and binding (hybridisation) equilibria indicated in Equation (1), the binding constant ratio between Fc^+DNA and FcDNA (K_{ox}/K_{red}) was calculated to be *c.* 23 from $E_b^{\circ\prime} - E_f^{o\prime} (= \Delta E_a^{o\prime})$ for the duplex **FcMd14/cd14**. It means that the oxidation of **FcMd14** facilitates its hybridisation with **cd14** for 23 times in the binding constant (*39*, *40*). If multiple Fc units were introduced into a conjugate, more distinct regulation of binding would be possible by electric field control

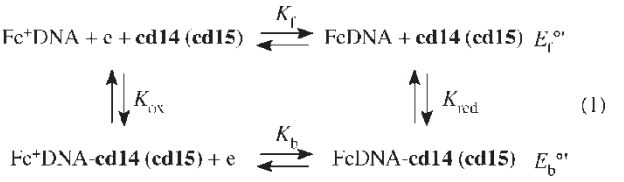

$$E_b^{o\prime} - E_f^{o\prime} = (RT/F)\ln(K_f/K_b) = (RT/F)\ln(K_{ox}/K_{red}).$$

The oxidation potential of the Fc units in **FcSh8**, **FcMh6** and **FcLh6** shifted to positive side when they formed hairpin structures. This is not due to the effect of temperature, because the potential shift was marginal for the FcDNA with a control sequence that cannot form a hairpin structure (data not shown). The positive shift in the potential of Fc oxidation means that the formation of Fc^+ is not preferable in the microenvironment, where Fc exists. It is quite reasonable, because the Fc units should be located on the top of hydrophobic core of base-pair stacking. Here, we cannot evaluate the value of K_{ox}/K_{red} for hairpin formation, because we had to do CV measurements at different temperatures to estimate the $E^{o\prime}$s for the states of coil and hairpin. Nevertheless, especially for **FcMh6**, a hairpin-coil equilibrium could be moved by the control of applied voltage to some extent.

In summary, we prepared three Fc amidite reagents with different chain lengths and built them into oligonucleotide backbones to form several FcDNA conjugates that form duplexes or hairpin structures. While the Fc units in duplex backbones destabilised the structures, those in hairpin loops could stabilise hairpin structures, if the chain length is appropriate. The shifts in oxidation potentials of the Fc units were opposite each other for duplexes and hairpins; the potentials of Fc in duplex and hairpin loop shifted to negative and positive sides, respectively. This would be explained by the difference in hydrophilicity of the microenvironments, where each Fc is located. Fc built in DNA backbone could be used as a probe for the second structures of nucleic acids. In addition, these results would show the possibility of electrochemical regulation of the second structure of nucleic acids.

Table 3. The shifts in oxidation potentials when forming the structures.

	$\Delta E_a^{o\prime}$/mV		
	Duplex[a]		
Fc units	with **cd14**	with **cd15**	Hairpin[b]
FcS	−30	−12	+47
FcM	−74	−55	+83
FcL	−55	−22	+55

[a] Potential shift: $E_{duplex}^{o\prime} - E_{coil}^{o\prime}$ ($E_b^{o\prime} - E_f^{o\prime}$ in Equation (1)).
[b] Potential shift: $E_{hairpin}^{o\prime} - E_{coil}^{o\prime}$.

Experimental

General

400 MHz ^{1}H and 100 MHz ^{13}C NMR spectra were measured on an EX400 spectrometer (JEOL) at 298K. ^{31}P NMR spectrum was measured on a Unity Inova 400 (Brucker). Chemical shifts (δ) are expressed in ppm relative to $SiMe_4$ for ^{1}H and ^{13}C, and phosphate for ^{31}P NMR. Multiplicities are indicated as the following: s (singlet); d (doublet); dd (double doublets); dt (double triplets); t (triplet); q (quartet); m (multiplet). ^{1}H NMR coupling constants (J) are reported in Hz. IR spectra were collected on an FT-IR Spectrum one spectrometer (Perkin-Elmer). Elemental analysis was performed on a CHN Corder MT-6 (Yanaco). Matrix-assisted laser desorption ionisation mass spectrometry measurements (MALDI-TOF/MS) were carried out using a Voyager RP mass spectrometer (PerSeptive). Electrospray ionisation-time of flight mass spectrometry (ESI-TOF/MS) measurements of Fc amidites were carried out using a solution of acetonitrile saturated with lithium chloride with a LCT spectrometer (Micromass) in positive ion mode (*41*). The purities of all compounds were estimated to be $>99\%$ from their NMR spectra.

Synthesis of Fc amidites

*Fc dialdehyde (**2**)*

Fc (3.5 g, 19 mmol) and *N*,*N*,*N*′,*N*′-tetramethylethylenediamine (TMEDA; 2.7 g, 23 mmol) were dissolved in hexane (21 ml) under an atmosphere of argon. To the solution, a hexane solution of *n*-butyllithium (1.6 M, 30 ml, 47 mmol) was added slowly via an addition funnel in 30 min. The solution was stirred for 24 h at room temperature. The solution changed its colour from dark orange to dark brown with yellow precipitate. To the suspension, a THF solution of DMF [5.2 ml (67 mmol) in 30 ml THF] was added slowly via an addition funnel in 1 h at -78°C (acetone–dry ice) and then stirred for 22 h at room temperature. The solution gave a black precipitates. The reaction was quenched by an addition of deionised water in ice bath. The organic phase was diluted with ethyl acetate, dried with anhydrous $MgSO_4$ and concentrated *in vacuo*. The residue was subjected to silica gel column chromatography (hexane–ethyl acetate: 3/2 v/v) and the fraction of R_f 0.26 was collected (*25*, *26*).

Yield 76% (3.5 g, 14 mmol); dark red solid; ^{1}H NMR (400 MHz, $CDCl_3$) δ 9.95 (s, 2H, CHO), 4.89 (t, $J = 2.0$ Hz, 4H, Fc), 4.68 (t, $J = 2.0$ Hz, 4H, Fc) ppm; ^{13}C NMR (100 MHz, $CDCl_3$) δ 192.8 (CHO), 74.13, 71.15, 70.83 ppm; IR (KBr) ν 1684, 1664, 1456, 1372, 1246, 1040, 745 cm^{-1}; MS (MALDI) *m*/*z* calculated for $C_{12}H_{10}FeO_2^+$ ([M+H]$^+$): 243.05, found: 243.27.

*Fc unsaturated diester (**3**)*

Fc dialdehyde **2** (4.3 g, 18 mmol) and diethyl phosphonoacetate (8.4 g, 37 mmol) were dissolved in THF (28 ml) under an atmosphere of argon. To the solution, sodium hydride (1.5 g, 37 mmol) was added in five aliquots at 0°C in 1 h and stirred for 4 h at room temperature. The reaction was quenched by an addition of deionised water in water bath. The organic phase was diluted with ethyl acetate (30 ml), washed with deionised water and brine, dried with anhydrous $MgSO_4$ and concentrated *in vacuo*. The residue was subjected to silica gel column chromatography (hexane–ethyl acetate: 3/1 v/v) and the fraction of R_f 0.49 was collected (*27*).

Yield 97% (7.2 g, 19 mmol); dark red solid; ^{1}H NMR (400 MHz, $CDCl_3$) δ 7.40 (d, $J = 16$ Hz, 2H, Fc—CH), 5.98 (d, $J = 16$ Hz, 2H, CHCO), 4.45 (d, $J = 2.0$ Hz, 4H, Fc), 4.38 (t, $J = 2.0$ Hz, 4H, Fc), 4.22 (q, $J = 6.8$ Hz, 4H, OCH_2), 1.33 (t, $J = 6.8$ Hz, 6H, CH_3) ppm; ^{13}C NMR (100 MHz, $CDCl_3$) δ 166.9 (C═O), 143.8, 116.3, 80.0, 72.3, 69.8, 60.2, 14.3 ppm; IR (KBr) ν 1720, 1637, 1368, 1305, 1197, 1166, 1039 cm^{-1}; MS (MALDI) *m*/*z* calculated for $C_{20}H_{22}FeO_4^+$ ([M+H]$^+$): 383.23, found: 383.36.

*Fc saturated diester (**4**)*

3 (0.5 g, 1.3 mmol) and copper chloride (CuCl, 0.5 g, 5 mmol) were dissolved in methanol (26 ml) under an atmosphere of argon. To the solution, sodium borohydride (1 g, 26 mmol) was added at 0°C in 30 min and stirred for 1 h in ice bath. The colour of the solution changed from dark red to dark green. Copper chloride (0.30 g, 3 mmol) and sodium borohydride (0.30 g, 7.7 mmol) were added again into the solution in ice bath and the solution was stirred further for 6 h. The colour of the solution turned yellow. The solution was filtered and 5% HCl was added to the filtrate to form a yellow solid. The solid was dissolved in ethyl acetate (30 ml). The solution was washed with saturated $NaHCO_3$ (10 ml) and brine (10 ml), dried with anhydrous Na_2SO_4 and concentrated *in vacuo*. The residue was subjected to silica gel column chromatography (hexane–ethyl acetate: 5/1 v/v) and the fraction of R_f 0.46 was collected (*28*, *29*).

Yield 84% (0.42 g, 1.1 mmol); yellow oil; ^{1}H NMR (400 MHz, $CDCl_3$) δ 4.14 (q, $J = 7.1$ Hz, 4H, OCH_2), 4.01 (s, 8H, Fc), 2.68–2.63 (m, 4H, $FcCH_2$), 2.54–2.49 (m, 4H, CH_2CO), 1.26 (t, $J = 7.3$ Hz, 6H, CH_3) ppm; ^{13}C NMR (100 MHz, $CDCl_3$) δ 173.0 (C═O), 87.5, 68.5, 68.1, 60.3, 35.9, 24.7, 14.2 ppm; IR (KBr) ν 2926, 1737, 1178 cm^{-1}; MS (MALDI) *m*/*z* calculated for $C_{20}H_{26}FeO_4^+$ ([M+H]$^+$): 387.26, found: 387.34.

*Fc dipropanol (**5**)*

A solution of LAH (0.08 g, 2.1 mmol) in anhydrous THF (4 ml) was prepared under an atmosphere of argon and

stirred for 10 min at room temperature. To the mixture, a THF solution of **4** (0.40 g (1 mmol) in 8 ml THF) was added drop by drop via an addition funnel in 1 h, keeping the solution refluxed, then the solution was refluxed further for 4 h. Ethyl acetate (40 ml) and deionised water (2.1 ml) were added slowly to the solution in this order in an ice bath to quench the reaction. After stirring with 0.2 M HCl (10 ml) for 1 h, the solution was extracted with ethyl acetate (40 ml ×3). The organic phase was washed with deionised water (10 ml) and brine (10 ml), dried with anhydrous Na_2SO_4 and concentrated *in vacuo*. The residue was subjected to silica gel column chromatography (hexane–ethyl acetate: 1/3 v/v) and the fraction of R_f 0.51 was collected (*30*).

Yield 84% (0.34 g, 0.87 mmol); red yellow oil; ^{1}H NMR (400 MHz, $CDCl_3$) δ 4.02 (s, 8H, Fc), 3.65 (t, $J = 6.8$ Hz, 4H, CH_2OH), 2.39 (t, $J = 7.8$Hz, 4H, $FcCH_2$), 1.75 (dt, $J = 7.8$, 6.8 Hz, 4H, $FcCH_2CH_2$) ppm; ^{13}C NMR (100 MHz, $CDCl_3$) δ 88.5, 68.7, 67.8, 62.5, 34.05, 25.6 ppm; IR (KBr) ν 3360, 3088, 2938, 2875, 1472, 1446, 1040, 1021, 825, 490 cm^{-1}; MS (MALDI) *m/z* calculated for $C_{16}H_{22}FeO_2^+$ ($[M+H]^+$): 303.19, found: 303.42.

*Monotrityl Fc (**6**)*

Fc diol, **5** (0.20 g, 0.65 mmol) and 4-dimethylaminiopyridine (DMAP; 0.016 g, 0.13 mmol) were dissolved in 5 ml dry THF under an argon atmosphere. The solution was evaporated *in vacuo*. This procedure was repeated again. The residue and *N*,*N*-diisopropylethylamine (DIPEA; 0.11 ml, 0.65 mmol) was dissolved in dry THF (5 ml) under an atmosphere of argon. To the solution, DMTr-Cl (0.24 g, 0.72 mmol) was added and stirred for 4 h at room temperature. The reaction was quenched with methanol (2 ml) and the solution was concentrated *in vacuo*. The residue was dissolved in dichloromethane (40 ml) and washed with saturated $NaHCO_3$ (5 ml). The organic phase was dried with anhydrous Na_2SO_4 and concentrated *in vacuo*. The residue was subjected to silica gel column chromatography (hexane–ethyl acetate: 2/1 v/v) and the fraction of R_f 0.29 was collected. Silica gel was deactivated with 1% triethylamine in hexane–ethyl acetate 2/1 before chromatography (*31*).

Yield 46% (0.18 g, 0.30 mmol); yellow oil; ^{1}H NMR (400 MHz, $CDCl_3$) δ 7.46–7.17 (m, 9H, DMTr), 6.82 (d, $J = 8.8$ Hz, 4H, DMTr), 3.99–3.92 (m, 8H, Fc), 3.77 (s, 6H, DMTr), 3.62 (t, $J = 6.8$ Hz, 2H, CH_2OH), 3.10 (t, $J =$ 5.8 Hz, 2H, CH_2ODMTr), 2.39 (t, $J = 7.8$ Hz, 4H, $FcCH_2$), 1.85–1.71 (m, 4H, $FcCH_2CH_2$) ppm; ^{13}C NMR (100 MHz, $CDCl_3$) δ 158.3, 145.3, 136.6, 130.0, 128.2, 127.6, 126.5, 112.9, 88.9, 88.3, 85.7, 68.6, 68.4, 67.9, 67.6, 63.1, 62.5, 55.1, 34.1, 31.4, 25.9, 25.7 ppm; MS (MALDI) *m/z* calculated for $C_{37}H_{40}FeO_4^+$ ($[M+H]^+$): 605.56, found: 607.02.

*Fc amidite (**7**)*

Monotrityl Fc, 6 (0.17 g, 0.28 mmol) was dissolved in dry acetonitrile (3 ml) under an atmosphere of argon. To the solution, DIPEA (0.15 ml, 0.84 mmol) and chloro(diisopropylamino)(β-cyanoethoxy)phosphine (0.13 ml, 0.56 mmol) was added in this order and the solution was stirred for 30 min at room temperature. The reaction mixture was directly subjected to silica gel column chromatography (hexane–ethyl acetate–triethylamine: 200/100/1 v/v/v) and the component of R_f 0.51 was collected (*27*).

Yield 83% (0.19 g, 0.23 mmol); yellow oil; ^{1}H NMR (400 MHz, $CDCl_3$) δ 7.46–7.20 (m, 9H, DMTr), 6.85–6.80 (m, 4H, DMTr), 3.98–3.91 (m, 8H, Fc), 3.84–3.76 (m, 8H, DMTr, CH_2CH_2CN), 3.67–3.58 (m, 4H, CH_2OP, NCH), 3.09 (t, $J = 6.8$ Hz, 2H, CH_2ODMTr), 2.60 (t, $J = 6.8$ Hz, 2H, CH_2CN), 2.42–2.37 (m, 4H, $FcCH_2$), 1.84–1.80 (m, 4H, $FcCH_2CH_2$), 1.20–1.17 (m, 12H, CH_3) ppm; ^{13}C NMR (100 MHz, $CDCl_3$) δ 158.3, 145.3, 136.7, 123.0, 128.2, 127.7, 126.6, 117.6, 113.0, 88.8, 88.3, 85.7, 68.6, 68.5, 67.8, 67.8, 63.3, 63.1, 58.4, 55.2, 42.9, 32.7, 31.4, 26.0, 25.7, 24.6, 20.4 ppm; MS (ESI) *m/z* calculated for $C_{46}H_{57}FeN_2O_5P^+$ ($[M+Li]^+$): 811.35, found: 811.42.

*Iodoethanol DMTr (**8**)*

2-Iodoethanol (1 g, 5.8 mmol) was dissolved in dry THF (20 ml) under an atmosphere of argon. DMTr-Cl (2.4 g, 7 mmol) and triethylamine (2 ml, 14 mmol) were added in this order to the solution and stirred for 14 h at room temperature. The solution changed its colour from red to yellow and then white precipitate appeared. The suspension was diluted with ethyl acetate (30 ml) and washed with saturated $NaHCO_3$ (10 ml) and brine (10 ml) in this order. The organic phase was dried with anhydrous Na_2SO_4, filtered, and the filtrate was concentrated *in vacuo*. The residue was subjected to silica gel column chromatography (hexane–ethyl acetate: 7/1 v/v) and the fraction of R_f 0.37 was collected (*21*, *42*).

Yield 99% (2.7 g, 5.8 mmol); colourless oil; ^{1}H NMR (400 MHz, $CDCl_3$) δ 7.47–7.20 (m, 9H, DMTr), 6.85–6.82 (m, 4H, DMTr), 3.79 (s, 6H, DMTr), 3.38 (t, $J = 7.0$ Hz, 2H, I—CH_2CH_2), 3.16 (t, $J = 7.0$ Hz, 2H, I—CH_2CH_2) ppm; ^{13}C NMR (100 MHz, $CDCl_3$) δ 158.5, 144.8, 136.1, 130.0, 128.1, 127.8, 126.8, 113.1, 86.4, 64.2, 55.2, 39.3 ppm.

*Monotrityl Fc (**9**)*

Fc diol, **5** (0.55 g, 1.8 mmol) was dissolved in dry THF (5 ml) under an argon atmosphere. Sodium hydride (0.27 g, 6.8 mmol) and 15C5 (1.1 ml, 5.4 mmol) were added into the solution and stirred for 5 min at room temperature. To the solution, a dry THF solution of iodoethyl DMTr (**8**)

(1.9 g, 4 mmol in 40 ml THF) was added and refluxed for 37 h. The colour of the solution changed from yellow to brown. The reaction was quenched with deionised water (10 ml) and the solution was extracted with dichloromethane (50 ml). The organic phase was dried with anhydrous Na_2SO_4 and concentrated *in vacuo*. The residue was subjected to silica gel column chromatography (hexane–ethyl acetate: 3/1 v/v) and the fraction of R_f 0.29 was collected (*21*, *42*).

Yield 44% (0.52 g, 0.80 mmol); yellow oil; ^{1}H NMR (400 MHz, $CDCl_3$) δ 7.50–7.18 (m, 9H, DMTr), 6.83 (d, $J = 8.8$ Hz, 4H, DMTr), 3.99 (d, $J = 5.9$ Hz, 8H, Fc), 3.78 (s, 6H, DMTr), 3.67–3.58 (m, 4H, OCH_2CH_2O), 3.49 (t, $J = 6.3$ Hz, 2H, CH_2OH), 3.23 (t, $J = 5.1$ Hz, 2H, $CH_2OCH_2CH_2$), 2.46–2.35 (m, 4H, CH_2—Fc—CH_2), 1.87–1.68 (m, 4H, $CH_2CH_2OCH_2$, CH_2CH_2OH) ppm; ^{13}C NMR (100 MHz, $CDCl_3$) δ 158.3, 145.1, 136.3, 130.0, 128.2, 127.7, 126.6, 113.0, 88.5, 87.8, 85.9, 70.6, 70.5, 68.6, 67.9, 64.1, 63.3, 62.5, 60.3, 55.1, 30.0, 25.7, 22.6, 20.9 ppm; MS (MALDI) *m/z* calculated for $C_{39}H_{44}FeO_5^+$ ($[M+H]^+$): 649.61, found: 650.85.

*Fc amidite (**10**)*

Fc amidite, **10** was synthesised according to the procedure in Fc amidite, **7** (*27*).

Yield 84% (0.25 g, 0.29 mmol); yellow oil; ^{1}H NMR (400 MHz, $CDCl_3$) δ 7.49–7.15 (m, 9H, DMTr), 6.82 (d, $J = 7.8$ Hz, 4H, DMTr), 3.98 (d, $J = 6.8$ Hz, 8H, Fc), 3.84–3.77 (m, 8H, DMTr, CH_2CH_2CN), 3.66–3.60 (m, 6H, CH_2OP, CH_2CH_2ODMTr, $NCHCH_3$), 3.48 (t, $J = 5.8$ Hz, 2H, CH_2OCH_2), 3.22 (t, $J = 4.9$ Hz, 2H, CH_2ODMTr), 2.61 (t, $J = 5.9$ Hz, 2H, CH_2CN), 2.50–2.37 (m, 4H, $FcCH_2$), 1.79 (t, $J = 6.8$ Hz, $FcCH_2CH_2$), 1.25–1.81 (m, 12H, $NCHCH_3$) ppm; ^{13}C NMR (100 MHz, $CDCl_3$) δ 158.3, 145.1, 136.3, 130.0, 128.2, 127.7, 126.6, 117.6, 113.0, 88.5, 88.3, 85.9, 70.7, 70.2, 68.7, 68.6, 67.9, 67.8, 63.3, 63.1, 58.1, 55.1, 42.9, 32.6, 31.3, 25.9, 25.7, 24.6, 20.3 ppm; ^{31}P NMR (162 MHz, $CDCl_3$) δ 145.586 (P) ppm; MS (ESI) *m/z* calculated for $C_{48}H_{61}FeN_2O_6P^+$ ($[M+Li]^+$): 855.38, found: 854.99.

*Bromoethanol DMTr (**11**)*

Bromoethanol DMTr (**11**) was synthesised from bromoethanol and DMTr-Cl according to the procedure of **8** (*21*, *42*).

Yield 100% (3.4 g, 8 mmol); colourless oil; ^{1}H NMR (400 MHz, $CDCl_3$) δ 7.47–7.19 (m, 9H, DMTr), 6.84–6.81 (m, 4H, DMTr), 3.79 (s, 6H, DMTr), 3.46–3.38 (m, 4H, Br—CH_2CH_2O) ppm; ^{13}C NMR (100 MHz, $CDCl_3$) δ 158.5, 144.7, 135.9 130.0, 128.1, 127.8, 126.8, 113.2, 86.2, 63.6, 55.2, 31.2 ppm.

*Ditrityl Fc (**12**)*

Fc diol, **5** (0.11 g, 0.40 mmol) was dissolved in dry THF (5 ml) under an argon atmosphere. Sodium hydride (0.06 g, 1.5 mmol) and 15C5 (0.23 ml, 1.1 mmol) were added into the solution and stirred for 10 min at room temperature. To the solution, a dry THF solution of bromoethyl DMTr (**11**) (0.47 g, 1.1 mmol in 2.2 ml THF) was added and refluxed for 25 h. The colour of the solution changed from yellow to brown. The reaction was quenched with methanol (0.04 ml) and the solution was diluted with ethyl acetate. The solution was washed with deionised water (5 ml) and brine (5 ml) in this order. The organic phase was dried with anhydrous Na_2SO_4 and concentrated *in vacuo*. The residue was subjected to silica gel column chromatography (hexane–ethyl acetate: 4/1 v/v) and the fraction of R_f 0.29 was collected (*32–35*).

Yield 42% (0.15 g, 0.15 mmol); yellow oil; ^{1}H NMR (400 MHz, $CDCl_3$) δ 7.50–7.15 (m, 18H, DMTr), 6.82–6.80 (m, 8H, DMTr), 3.98 (d, $J = 9.8$ Hz, 8H, Fc), 3.74 (s, 12H, DMTr), 3.59 (t, 4H, $J = 5.8$ Hz, CH_2CH_2-ODMTr), 3.45 (t, $J = 6.8$ Hz, 4H, $CH_2OCH_2CH_2O$), 3.22 (t, $J = 4.9$ Hz, 4H, OCH_2CH_2DMTr), 2.44–2.40 (m, 4H, Fc—CH_2), 1.81–1.74 (m, 4H, Fc-$CH_2CH_2CH_2$) ppm; ^{13}C NMR (100 MHz, $CDCl_3$) δ 158.4, 141.5, 136.4, 130.1, 128.3, 127.7, 126.6, 113.0, 88.5, 85.9, 70.8, 70.3, 68.7, 67.9, 63.3, 55.2, 31.3, 25.9 ppm; MS (ESI) *m/z* calculated for $C_{62}H_{66}FeO_8^+$ ($[M+H]^+$): 996.03, found: 995.47.

*Monotrityl Fc (**13**)*

Ditrityl Fc, **12** (0.11 g, 0.11 mmol) was dissolved in 5% (v/v) water in acetonitrile (5 ml) under an argon atmosphere and stirred for 5 min. To this solution, ceric triflate (16 mg, 0.02 mmol) was added and stirred for 20 h at room temperature. The solution turned red immediately and gradually changed to green. The solution was concentrated *in vacuo*. The residue was subjected to silica gel column chromatography (hexane–ethyl acetate: 3/2 v/v) and the fraction of R_f 0.30 was collected (*36*).

Yield 91% (0.067 g, 0.097 mmol); yellow oil; ^{1}H NMR (400 MHz, $CDCl_3$) δ 7.49–6.76 (m, 13H, DMTr), 4.04 (br, 8H, Fc), 3.78 (s, 6H, DMTr), 3.71 (t, $J = 4.9$ Hz, 2H, CH_2CH_2OH), 3.63–3.60 (m, 2H, CH_2CH_2ODMTr), 3.52–3.49 (m, 4H, Fc—$CH_2CH_2CH_2$), 3.46–3.43 (m, 2H, CH_2CH_2ODMTr), 3.22 (t, $J = 4.9$ Hz, 2H, CH_2CH_2-OH), 2.44–2.33 (m, 4H, CH_2—Fc—CH_2), 1.77 (dt, $J = 7.8$, 6.8 Hz, 4H, CH_2CH_2—Fc—CH_2CH_2) ppm; ^{13}C NMR (100 MHz, $CDCl_3$) δ 158.3, 145.1, 136.4, 130.1, 128.2, 127.7, 126.6, 113.0, 88.6, 88.4, 85.9, 71.7, 70.7, 70.3, 68.8, 68.6, 67.9, 68.7, 67.9, 63.3, 61.8, 55.2, 31.3, 31.1, 25.9 ppm; MS (MALDI) *m/z* calculated for $C_{41}H_{48}FeO_6^+$ ($[M+H]^+$): 693.66, found: 693.52 (*36*).

*Fc Amidite (**14**)*

Fc amidite, **14** was synthesised according to the procedure in Fc amidite, **7** (*27*).

Yield 99% (0.075 g, 0.084 mmol); yellow oil; ^{1}H NMR (400 MHz, $CDCl_3$) δ 7.50–7.16 (m, 9H, DMTr), 6.24 (d, $J = 8.8$ Hz, 4H, DMTr), 3.99–3.96 (m, 8H, Fc), 3.86–3.76 (m, 10H, DMTr, CH_2CH$_2$CN, CH$_2$CH_2OP), 3.63–3.56 (m, 6H, CH_2O CH$_2$CH$_2$OP, CH_2CH$_2$ODMTr, NCHCH$_3$), 3.50–3.42 (m, 4H, CH_2OCH$_2$CH$_2$ODMTr, CH_2CH$_2$OP), 3.22 (t, $J = 4.9$ Hz, 2H, CH_2ODMTr), 2.64–2.61 (m, 2H, CH_2CN), 2.45–2.34 (m, 4H, FcCH_2), 1.80–1.73 (m, 4H, FcCH$_2$CH_2), 1.20–1.11 (m, 12H, NCHCH_3) ppm; ^{13}C NMR (100 MHz, $CDCl_3$) δ 158.3, 145.1, 136.4, 130.1, 128.2, 127.7, 126.6, 117.6, 113.0, 88.5, 88.5, 85.9, 70.8, 70.7, 70.7, 70.3, 68.7, 68.6, 68.5, 67.9, 63.3, 62.7, 58.4, 55.2, 43.0, 31.3, 31.2, 25.9, 25.8, 24.6, 20.3 ppm; ^{31}P NMR (162 MHz, $CDCl_3$) δ 143.847 (P) ppm; MS (ESI) *m/z* calculated for $C_{50}H_{65}FeN_2O_6P^+$ ([M+Li]$^+$): 883.41, found: 883.33.

Synthesis of FcDNA conjugates

ODNs were synthesised by a conventional phosphoramidite method on a universal CPG (controlled pore glass) column (Proligo) using an Expedite 8900 (Applied Biosystems, Foster City, CA, USA) DNA synthesizer. Cleavage from the CPG support and deprotection was carried out by incubation in aqueous ammonia (28%) for 8 h at 80°C. The aqueous ammonia was evaporated under reduced pressure. From these crude mixtures, the resulting ODNs were purified with conventional two-step procedure using RP-HPLC (linear gradient: 0.1 M triethylammonium acetate, pH 7/acetonitrile) and identified with MALDI-TOF/MS (*42*).

UV melting

Thermal denaturation experiments were carried out in phosphate buffer solutions (10 mM, pH 7) containing 100 mM KCl on a UV-1650 (Shimadzu, Kyoto, Japan) UV/vis spectrophotometer equipped with a Peltier thermal controller. Concentrations of each component of the duplexes or hairpins were 1 μM. Prior to the beginning of each melt, the samples were degassed at 85°C for 5 min and then annealed with slow cooling to 0°C. In the denaturation experiments, the solutions were heated at a rate of 0.5 deg min^{-1} after equilibration for 20 min at 0°C (*37*).

Cyclic voltammetry

Electrochemical behaviour of the synthesised FcDNAs was studied by CV using an Electrochemical Analyser (ALS 842B) with a dual Au comb electrode chip (BAS Au comb electrode). The chip consists of two working Au electrodes (65 pairs of generator (W_g) and collector (W_c): 10 μm width, 5 μm spacing, 2 mm length), an Au electrode, and an Ag/AgCl electrode as working, counter and reference electrodes, respectively. DNA solutions (20 μl) containing 10 μM each DNA component (10 mM phosphate buffer (pH 7), 100 mM KCl) were dropped onto the chip so as to cover all of the four electrodes and CV measurements were performed in a shield box (LS-5) equipped with a Peltier thermal controller. The potential of W_g was scanned at the rate of 10 mV s^{-1} from −0.2 to 0.6 V; W_c was kept constant at −0.2 V. The shifts in the potentials that gave the maxima of the first derivatives of the voltammograms in oxidation processes with W_g were summarised in Table 3 (*6*).

Acknowledgements

This work was partially supported by a Grant-in-Aid for Scientific Research (B) (20350038) from MEXT (T.I.). The authors are also grateful to the support from PRESTO, JST (T.I.).

References

(1) For example, Hermanson, G.T. *Bioconjugate Techniques*; Academic Press: San Diego, 1996.
(2) Agrawal, S., Ed. Methods in Molecular Biology, In *Protocols for Oligonucleotide Conjugates*; Humana Press: Totowa, 1994, Vol. 26.
(3) For example, Yamamoto, Y.; Uehara, A.; Tomita, T.; Komiyama, M. *Nucleic Acids Res.* **2004**, *32*, e153.
(4) For example, Madhavaiah, C.; Silverman, S.K. *J. Am. Chem. Soc.* **2008**, *130*, 2936–2937.
(5) For example, Okamoto, A.; Kanatani, K.; Saito, I. *J. Am. Chem. Soc.* **2004**, *126*, 4820–4827.
(6) For example, Ihara, T.; Maruo, Y.; Takenaka, S.; Takagi, M. *Nucleic Acids Res.* **1996**, *24*, 4273–4280.
(7) Takenaka, S.; Uto, Y.; Kondo, H.; Ihara, T.; Takagi, M. *Anal. Biochem.* **1994**, *218*, 436–443.
(8) Ihara, T.; Nakayama, M.; Murata, M.; Nakano, K.; Maeda, M. *Chem. Commun.* **1997**, 1609–1610.
(9) Nakayama, M.; Ihara, T.; Nakano, K.; Maeda, M. *Talanta* **2002**, *56*, 857–866.
(10) Ihara, T.; Nakayama, M.; Nakano, K.; Maeda, M. In *Biomedical Diagnostic Science and Technology*; Law, W.K., Akmal, N., Usmani, A.M., Eds.; Marcel Dekker: New York, 2002.
(11) Inouye, M.; Ikeda, R.; Takase, M.; Tsuri, T.; Chiba, J. *Proc. Natl Acad. Sci. USA* **2005**, *102*, 11606–11610.
(12) Zuo, X.; Song, S.; Zhang, J.; Pan, D.; Wang, L.; Fan, C. *J. Am. Chem. Soc.* **2007**, *129*, 1042–1043.
(13) Xiao, Y.; Qu, X.; Plaxco, K.W.; Heeger, A.J. *J. Am. Chem. Soc.* **2007**, *129*, 11896–11897.
(14) Wang, J.; Li, J.; Baca, A.J.; Hu, J.; Zhou, F.; Yan, W.; Pang, D.-W. *Anal. Chem.* **2003**, *75*, 3941–3945.
(15) Cahová, H.; Havran, L.; Brázdilová, P.; Pivonková, H.; Pohl, R.; Fojta, M.; Hocek, M. *Angew. Chem. Int. Ed.* **2008**, *47*, 2059–2062.
(16) Fojta, M.; Kostecka, P.; Trefulka, M.; Havran, L.; Palecek, E. *Anal. Chem.* **2007**, *79*, 1022–1029.
(17) Radi, A.-E.; O'Sullivan, C.K. *Chem. Commun.* **2006**, 3432–3434.

(18) Cheng, A.K.H.; Ge, B.; Yu, H.-Z. *Anal. Chem.* **2007**, *79*, 5158–5167.
(19) Zhang, Y.-L.; Huang, Y.; Jiang, J.-H.; Shen, G.-L.; Yu, R.-Q. *J. Am. Chem. Soc.* **2007**, *129*, 15448–15449.
(20) Xiao, Y.; Piorek, B.D.; Plaxco, K.W.; Heeger, A.J. *J. Am. Chem. Soc.* **2005**, *127*, 17990–17991.
(21) Ihara, T.; Shirasaka, Y.; Sato, Y.; Kitamura, Y.; Okada, K.; Tazaki, M.; Jyo, A. *Heterocycles* **2005**, *65*, 293–301.
(22) Willner, I.; Zayats, M. *Angew. Chem. Int. Ed.* **2007**, *46*, 6408–6418.
(23) Famulok, M.; Hartig, J.S.; Mayer, G. *Chem. Rev.* **2007**, *107*, 3715–3743.
(24) Mucic, R.C.; Herrlein, M.K.; Mirkin, C.A.; Letsinger, R.L. *J. Chem. Soc. Chem. Commun.* **1996**, 555–557.
(25) Federmam Neto, A.; Miller, J.; de Andrade, V.F.; Fujimoto, S.Y.; Afonso, M.M.F.; Archanjo, F.C.; Darin, V.A.; e Silva, M.L.A.; Borges, Á.D.L.; Ponte, G.D. *Anorg. Allg. Chem.* **2002**, *628*, 209–216.
(26) Fröhlich, R.F.G.; Zabelinskaja-Mackova, A.A.; Fechter, M.H.; Griengl, H. *Tetrahedron Asymm.* **2003**, *14*, 355–362.
(27) Navarro, A.-E.; Spinelli, N.; Moustrou, C.; Chaix, C.; Mandrand, B.; Brisset, H. *Nucleic Acids Res.* **2004**, *32*, 5310–5319.
(28) Brown, H.C.; Hess, H.M. *J. Org. Chem.* **1969**, *34*, 2206–2209.
(29) Debroy, P.; Naskar, D.; Roy, S. *Inorg. Chim. Acta* **2006**, *359*, 1215–1221.
(30) Gammill, R.B.; Gold, P.M.; Mizsak, S.A. *J. Am. Chem. Soc.* **1980**, *102*, 3095–3100.
(31) Ferreira, F.; Meyer, A.; Vasseur, J.-J.; Morvan, F. *J. Org. Chem.* **2005**, *70*, 9198–9206.
(32) Aspinall, H.C.; Greeves, N.; Lee, W.-M.; McIver, E.G.; Smith, P.M. *Tetrahedron Lett.* **1997**, *38*, 4679–4682.
(33) Greeves, N.; Lee, W.-M.; McLachlan, S.P.; Oakes, G.H.; Purdie, M.; Bickley, J.F. *Tetrahedron Lett.* **2003**, *44*, 9035–9038.
(34) Zhang, J.-X.; Labaree, D.C.; Hochberg, R.B. *J. Med. Chem.* **2005**, *48*, 1428–1477.
(35) Hong, Y.-R.; Gorman, C.B. *J. Org. Chem.* **2003**, *68*, 9019–9025.
(36) Khalafi-Nezhad, A.; Alamdari, R.F. *Tetrahedron* **2001**, *57*, 6805–6807.
(37) Kitamura, Y.; Ihara, T.; Tsujimura, Y.; Osawa, Y.; Sasahara, D.; Yamamoto, M.; Okada, K.; Tazaki, M.; Jyo, A. *J. Inorg. Biochem.* **2008**, 102, 1921–1931.
(38) Bard, A.J.; Faulkner, L.R. *Electrochemical Methods. Fundamentals and Applications*; John Wiley: New York, 1980.
(39) Carter, M.T.; Rodriguez, M.; Bard, A.J. *J. Am. Chem. Soc.* **1989**, *111*, 8901–8911.
(40) Takenaka, S.; Ihara, T.; Takagi, M. *J. Chem. Soc. Chem. Commun.* **1990**, 1485–1487.
(41) Kele, Z.; Kupihár, Z.; Kovács, L.; Janáky, T.; Szabó, P.T. *J. Mass Spectrom.* **1999**, *34*, 1317–1321.
(42) Letsinger, R.L.; Wu, T. *J. Am. Chem. Soc.* **1995**, *117*, 7323–7328.